Supplementary Material

Parallel Quantum Computation of Vibrational Dynamics

Ksenia Komarova[1], Hugo Gattuso[2], R.D. Levine[1,3,4] and F. Remacle[1,2*]

[1] The Fritz Haber Center for Molecular Dynamics and Institute of Chemistry, The Hebrew University of Jerusalem, Jerusalem 91904, Israel

[2] Theoretical Physical Chemistry, UR MolSys B6c, University of Liège, B4000 Liège, Belgium

[3] Department of Chemistry and Biochemistry and [4]Department of Molecular and Medical Pharmacology, David Geffen School of Medicine, University of California, Los Angeles, CA 90095, USA

Table of Contents

* Corresponding author: Francoise Remacle, fremacle@uliege.be

1. Computation of 2D maps for a dimer of QD's

1.1 Electronic structure of the dimers

We consider an ensemble of 2000 dimers made of two QD's drawn in an ensemble of 4000 size dispersed QD's with a mean diameter, $\bar{D}$ = 4.4 nm and a Gaussian size dispersion with σ = 5 % :

$$P(D) = \frac{1}{\sigma\sqrt{2\pi}} \exp\left(-\frac{(D-\bar{D})^2}{2\sigma^2} \right) \quad \text{(S1)}$$

The two QD's making the dimer are separated by dithiol propane ligands, which leads to a surface to surface distance of 0.55nm. Each dimer is made of not quite identical dots because of the size dispersion which leads to an ensemble of 2000 'quasi' homodimers.

The electronic structure of a single dimer is computed as in ref. (Gattuso et al., 2020a) and (Collini et al., 2020) using the effective mass and **k.p** approximations(Efros et al., 1996; Norris and Bawendi, 1996) to determine the hole and electron orbitals that are used to build the excitonic Hamiltonian. For each QD, we consider two holes (1S and 2S) and one electron (1S) orbitals to build the hole-electron pairs. We take into account the spin-orbit (SO) coupling for the two hole states, as well as Coulomb interactions and crystal field splittings, which leads to 24 fine structure excitons (hole-electron pairs) per dot.(Efros et al., 1996; Norris and Bawendi, 1996; Wong and Scholes, 2011)

As explained in the main text, the 24 excitons separate into four main bands of fine structure states. The energetic order of these bands depends on the relative strengths of the SO coupling and the 1S-2S energy gap, see refs. (Collini et al., 2019; Collini et al., 2020). For 4.4 nm QD, the 1S-2S gap is 0.14 eV. The SO coupling value was fitted from 2DES experimental spectra of single QD's of the same 4.4 nm diameter to 0.22 eV.(Collini et al., 2019) Therefore for this dot size, the order of the four bands arising from the SO coupling of the hole states is $1S_{3/2}, 2S_{3/2}, 1S_{1/2}, 2S_{1/2}$. Based in the allowed values of the projection of the total angular momentum F_z (hole ± electron angular momentum) on the reference axis, the $1S_{3/2}$ and $2S_{3/2}$ bands are made of 8 quasi degenerate fine structure states (F_z=±2,±1,0 and F_z=±1,0) split by crystal field and Coulomb intradot interactions, and the $1S_{1/2}$ and $2S_{1/2}$ of 4 ones (F_z=±1,0 and 0). Among those the F_z =±2 states are dark. The crystal field splitting is taken to be 25 meV(Wong and Scholes, 2011) which is about 5 times smaller and not resolved in 2DES spectroscopy. The 1S and 2S bands are also weakly coupled by Coulomb interband intradot

interactions. (Gattuso et al., 2020a). This coupling scheme leads to the Hamiltonian matrix shown in Figure S1A.

In the dimer, the levels of the two QD's are coupled by interdot Coulomb interactions. The effective interdot coupling, $V_{\text{inter}}/\Delta E$, is quite large because the two dots making the dimer are quasi identical, therefore the electronic levels on each dot are quasi degenerate.(Collini et al., 2020; Gattuso et al., 2020a) Each single dot band is split into a low(L) and a high (H) band by the interdot Coulomb coupling, which leads to eight bands of eigenstates states for each dimer, 48 excited electronic states in total. The interdot coupling is larger between 1S states (≈ 65 meV) than between 2S (≈50 meV) because of confinement effects. Its strength is smaller than both the SO coupling strength and the band gap between the 1S and the 2S states. The relative magnitude of the different couplings leads to the 8 band level structure of the eigenstates of the dimer sketched in Figure S1B.

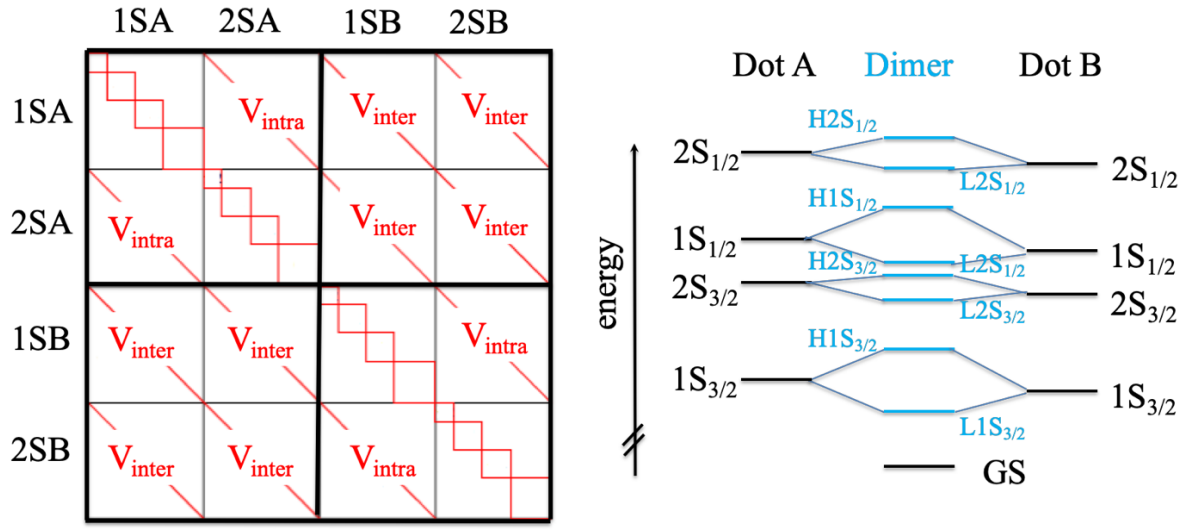

Figure S1 A. Structure of the Hamiltonian matrix in the zero order exciton basis. B: The 8 bands of fine structure eigenstates for a dimer made of 2 QD of not quite the same size because they are drawn from an ensemble of QD's of mean size 4.4 nm and 5% dispersion. The bands are $L1S_{3/2}$, $H1S_{3/2}$, $L2S_{3/2}$, $H2S_{3/2}$, $L1S_{1/2}$, $H1S_{1/2}$ and $L2S_{1/2}$ and $H2S_{1/2}$, L stands for 'low' and H for 'high'.

Since the two QDs that make each dimer are not identical, the states of each low and high branch in Figure S1B carry oscillator strength, with the states of the low band carrying less oscillator strength than those of the high one since these would be dark in the case of dimers made of identical dots.

We diagonalize the matrix shown in Figure S1A for an ensemble of 2000 dimers, made of two dots of slightly different sizes. For each dimer, we obtain 48 excited eigenstates. At the level of the ensemble, each transition frequency between excited eigenstates and the GS and between two excited states is therefore characterized by a mean value and a width which leads to inhomogeneous broadening.(Gattuso et al., 2020b) Eigenstates belonging to same of the 8 bands of states shown in Figure S1B have similar widths ranging from 17 meV for dimer eigenstates made of $L1S_{3/2}$ states to 40 meV for eigenstates made of $H2S_{1/2}$ states. The splitting between states of the low and high bands of $2S_{3/2}$, $L2S_{3/2}$ and $H2S_{3/2}$, is of the order of magnitude of the widths due to size dispersion which does not allow to resolve these bands in the absorption spectrum shown in Figure S2. The states of the $L1S_{1/2}$ band are also not resolved. They carry very little oscillation strength and merge with the states of the H2S3/2 band.

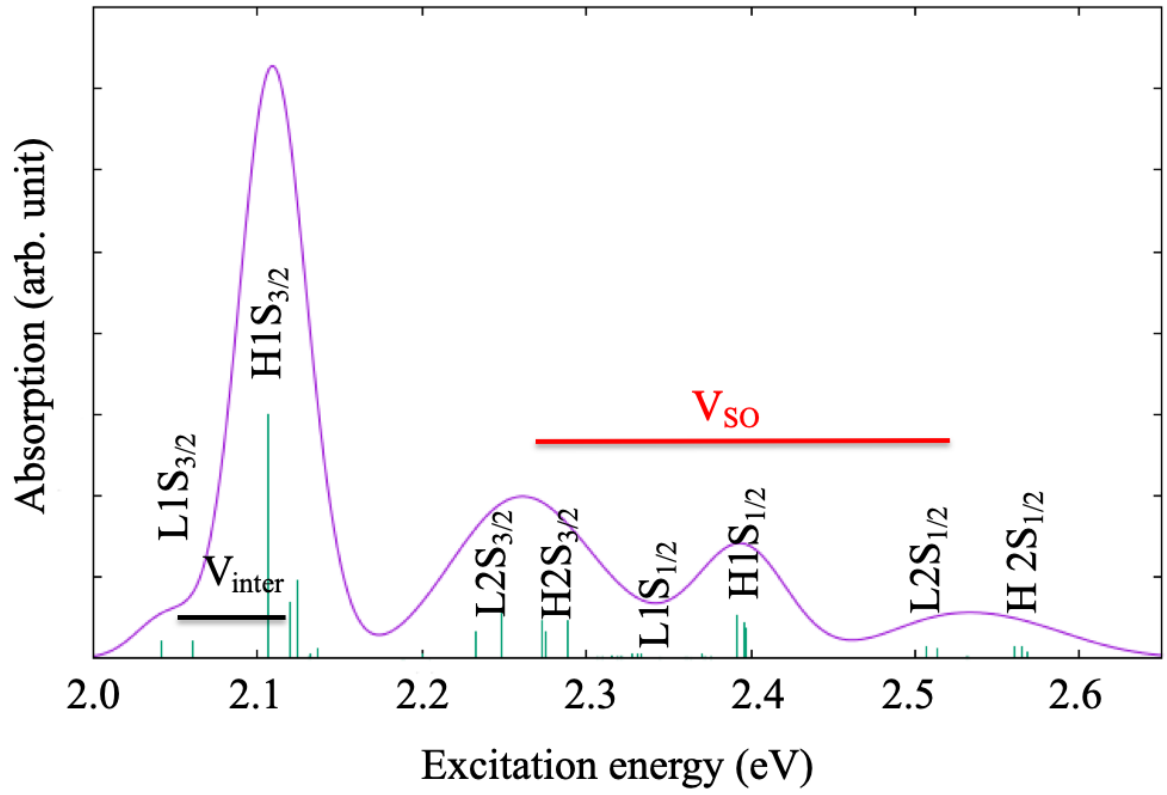

Figure S2 : Dimer absorption spectrum (Full line) computed for an ensemble of 2000 dimers (diameter = 4.4 nm, with 5 % size dispersion), taking into account the inhomogeneous width of each of the 48 eigenstates due to size dispersion. The underlying stick spectrum correspond to the mean value and mean transition dipole from the GS of each state over the ensemble. The magnitude of the SO coupling and of the Coulomb interdot coupling is shown.

1.2 Computation of the 2D maps

In the main text, we use electronic coherences between excited states of the dimer to emulate the quantum dynamics of two coupled harmonic oscillators. We have shown that these coherences can be probed by 2D electronic spectroscopy at room temperature in the solid state. The Hamiltonian model described in section S1.1 has been used to successfully characterize the electronic coherent response of QD of 4.4 nm diameter in solution(Collini et al., 2019) and of dimers of similar sizes in the solid state.(Collini et al., 2020)

The 2D maps reported in the main text are computed by third order perturbation theory in the impulsive limit for the duration of the three fs pulses involved in the rephasing phase matching direction. [ref mukamel, cho?] The phase matching directions are the macroscopic directions in which a signal is emitted after the interactions of the ensemble of dimers with three pulses separated by the time intervals τ, T and *t*. During each time interval, the populations in the eigenstates are stationary provided there is no population transfer due to vibronic coupling or induced by interactions with the environment, which is the case for the few dozens of fs time range considered here. We assume that the power of the laser pulse is weak enough that only one photon transitions are allowed from the GS. And that the carried frequency and duration of the pulse are such that all the excited states between 2 and 2.4 eV fall within the laser band width. As well documented and explained in the main text, there are 8 Liouvillian paths (shown graphically as double-sided Feynman diagrams in Figure S3) for each pair of excited states *i* and *j* that can be reached by a one photon transition to this band of states from the GS.

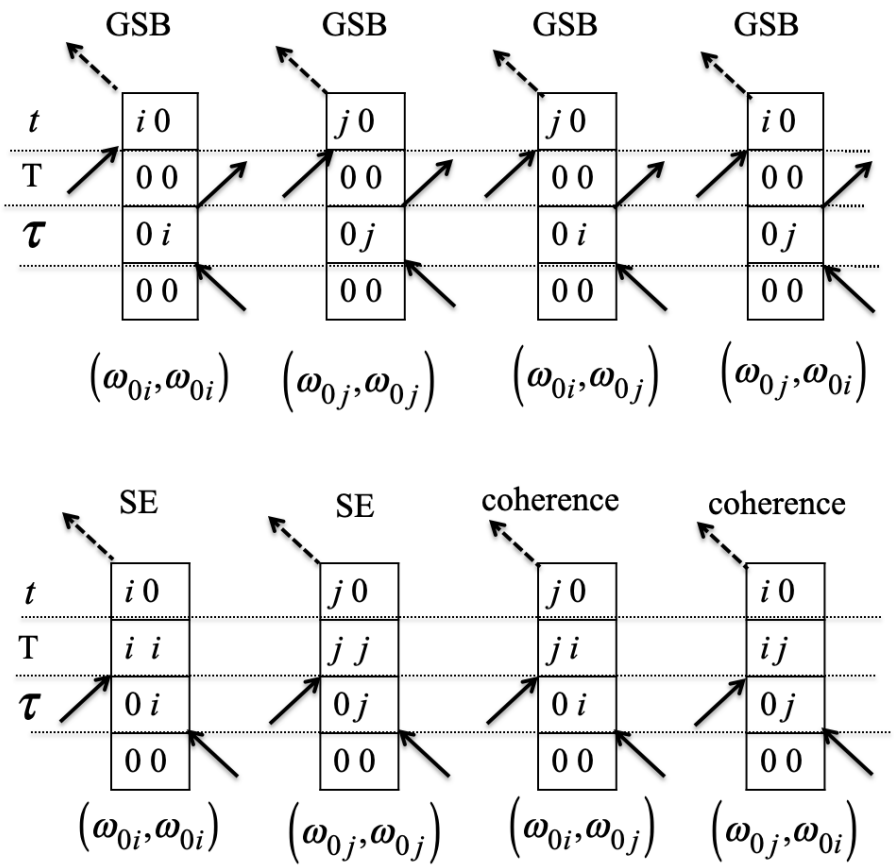

Figure S3. The 8 double sided Feynman diagrams that represents the 8 Liouvillian paths that contribute to the third order response in the rephasing phase matching direction for a pair of excited states reached by one photon transitions from the GS. (GSB (ground state bleaching, SE, stimulated emission). The three time intervals, τ between the first and the second pulse, T between the second and the third, and *t* from the third to emission, are indicated. Full arrows represents transitions due to the impulsive interaction with the electric field of the pulse and the dashed arrow emission after the third pulse. 00, 0*i*, etc.. are the index of the elements of the density matrix of the system, $|0\rangle\langle 0|, |0\rangle\langle i|$ etc... . For more details, see refs.(Mukamel, 1995; Cho, 2009) The frequency address of each path on a 2D map is reported.

The first pulse puts the systems in an excited state, creating a fast beating coherence with the GS during τ. After the interaction with the second pulse, during T, the systems can either be in the GS (GSB paths), in an excited state (SE paths) or in a coherence between two excited states. The interaction with the third pulse brings the system back in a coherence with the GS. The 2D maps are obtained by FT of the response along τ and *t* for specific values of T. The abscissa and ordinate of the map therefore corresponds to the transition frequencies from the GS, inhomogeneously broadened by the size dispersion as the absorption spectrum. Among the 8 paths shown in Figure S3, only the two coherence ones will exhibit a periodic time-dependence with respect to T, which corresponds to the transition frequency, ω_{ij}, between the

excited states i and j. They appear at the addresses $\left(\omega_{0i},\omega_{0j}\right)$ and $\left(\omega_{0j},\omega_{0i}\right)$ on the map. Two time-independent GSB path also contribute to these addresses. The two other GSB paths and the two SE paths contribute to the diagonal.

The 2D maps are computed by summing these 8 paths for each pair of the 48 excited states characterized by a mean transition frequency and a width as explained in section 1.1. A typical map with the addresses of the coherences is shown in figure S4. Non linear 2DES spectroscopy allows resolving the $LS_{3/2}$ and $HS_{3/2}$ bands that cannot be resolved in linear absorption spectroscopy because the coherences between excited states contributing to the off diagonal peaks have different periods. Because of the size dispersion, coherences between given bands of excited have slightly different periods, which allows a more precise mapping of the vibrational periods of the system that is emulated.

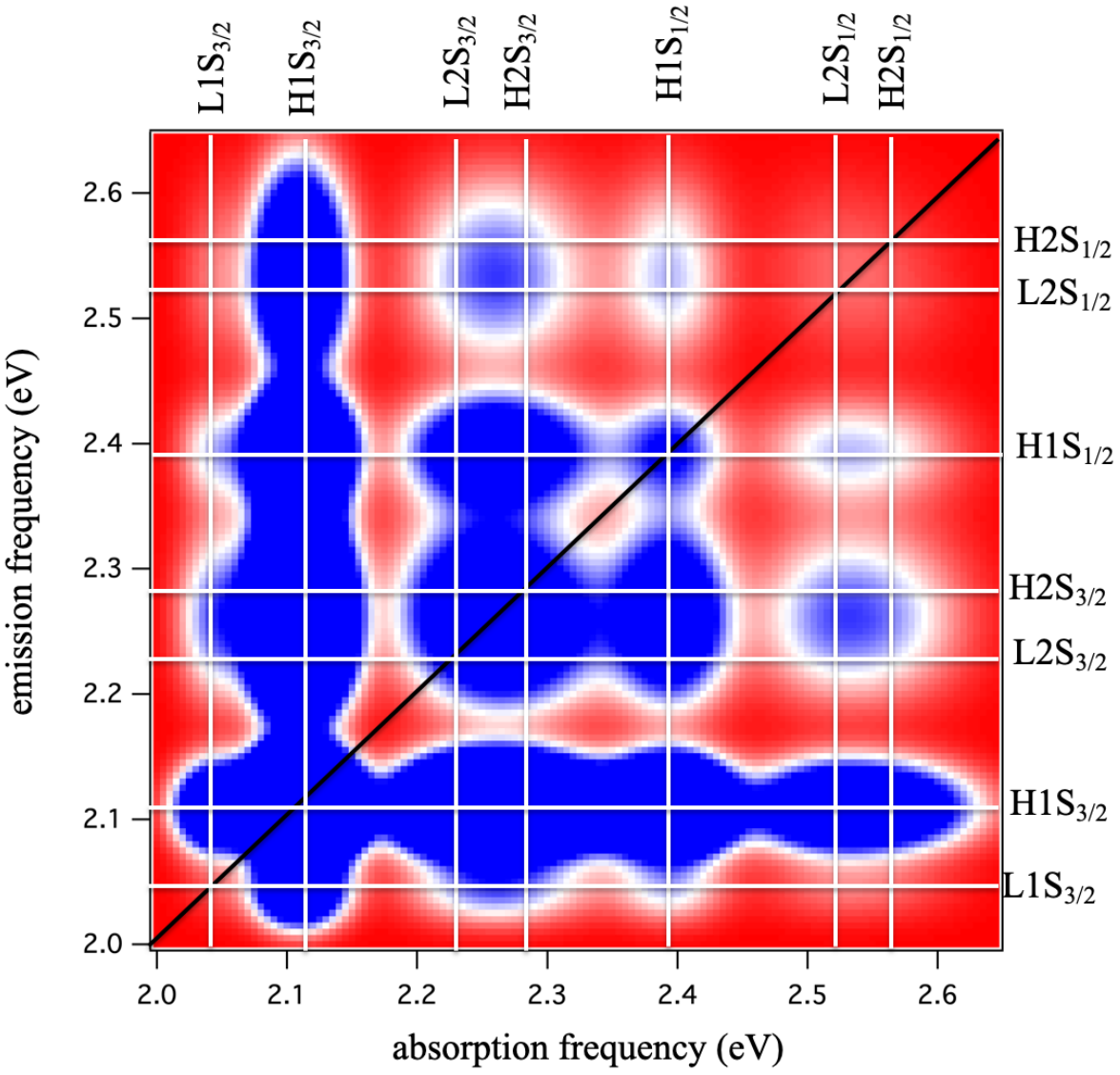

Figure S4. 2D ES map in the rephasing phase matching direction computed for T=0. The addresses of the peaks corresponding to the mean values of the transition frequencies are indicated.

References

Cho, M. (2009). *Two-Dimensional Optical Spectroscopy.* Boca Raton: CRC Press.

Collini, E., Gattuso, H., Bolzonello, L., Casotto, A., Volpato, A., Dibenedetto, C.N., et al. (2019). Quantum Phenomena in Nanomaterials: Coherent Superpositions of Fine Structure States in CdSe Nanocrystals at Room Temperature. *J. Phys. Chem. C* 123**,** 31286-31293. doi: 10.1021/acs.jpcc.9b11153.

Collini, E., Gattuso, H., Kolodny, Y., Bolzonello, L., Volpato, A., Fridman, H.T., et al. (2020). Room-Temperature Inter-Dot Coherent Dynamics in Multilayer Quantum Dot Materials. *J. Phys. Chem. C***,** https://doi.org/10.1021/acs.jpcc.1020c05572. doi: 10.1021/acs.jpcc.0c05572.

Efros, A.L., Rosen, M., Kuno, M., Nirmal, M., Norris, D.J., and Bawendi, M. (1996). Band-edge exciton in quantum dots of semiconductors with a degenerate valence band: Dark and bright exciton states. *Phys. Rev. B* 54(7)**,** 4843-4856. doi: 10.1103/PhysRevB.54.4843.

Gattuso, H., Fresch, B., Levine, R.D., and Remacle, F. (2020a). Coherent Exciton Dynamics in Ensembles of Size-Dispersed CdSe Quantum Dot Dimers Probed via Ultrafast Spectroscopy: A Quantum Computational Study. *Appl. Sci.* 10(4)**,** 1328. doi: 10.3390/app10041328.

Gattuso, H., Levine, R.D., and Remacle, F. (2020b). Massively Parallel Classical Logic via Coherent Dynamics of an Ensemble of Quantum Systems with Dispersion in Size. *Proc. Natl. Acad. Sci. USA***,** accepted.

Mukamel, S. (1995). *Principle of non linear optical spectroscopy.* Oxford: Oxfrod University Press.

Norris, D.J., and Bawendi, M.G. (1996). Measurement and assignment of the size-dependent optical spectrum in CdSe quantum dots. *Phys. Rev. B* 53(24)**,** 16338-16346. doi: 10.1103/PhysRevB.53.16338.

Wong, C.Y., and Scholes, G.D. (2011). Using two-dimensional photon echo spectroscopy to probe the fine structure of the ground state biexciton of CdSe nanocrystals. *J. Lumin.* 131(3)**,** 366-374. doi: http://dx.doi.org/10.1016/j.jlumin.2010.09.015.